Ship-induced effects on bottom-mounted acoustic current meters in shallow seas

Hans van Haren

Royal Netherlands Institute for Sea Research (NIOZ), P.O. Box 59, 1790 AB Den Burg, the Netherlands

ABSTRACT

The echo-amplitude of a 23-m-deep bottom-mounted acoustic Doppler current profiler (ADCP) shows regular spikes up to 30 dB above background level when a ship passes nearby, due to deep penetration of bubble clouds. This is evidenced from regularly occurring spikes in echo-data that are simultaneous with ferry crossings in a narrow sea-strait. The bubbles can nearly reach the bottom and are comparable in magnitude to near-bottom scattering off suspended material in vigorous tidal currents exceeding $1 \, \mathrm{m \, s^{-1}}$ in magnitude. The bubble clouds mask the sea surface from the echo-amplitude, which hampers the use of an ADCP for estimating atmospheric parameters and near-surface currents, under such conditions. The echo-spikes associated with the ferry are confirmed with coinciding dips in bottom pressure up to $1200 \, \mathrm{N \, m^{-2}}$ and with deviations up to $10°$ in the ADCP's heading due to pressure waves and magnetic field disturbances from under the ferry and from its rear, respectively.

© 2009 Elsevier Ltd. All rights reserved.

1. Introduction

A convenient way of making moored current observations in shallow seas and estuaries is by mounting an acoustic Doppler current profiler (ADCP) in a bottom-frame. An ADCP measures vertical profiles of all three components $[u, v, w]$ of water velocity or current as averages over the spread of its four beams that are slanted at an acute angle $\theta = 20°$ to the vertical. It also measures 'echo intensity amplitudes' in each of its beams (RDI, 1996). Bottom-mounting minimizes potential measurement errors due to instrument motions, compared to mooring-line or buoy-mounted instruments. It also avoids shipping hazards to some extent. For a typical shallow water instrument of nominally 2400–600 kHz transmit frequency, profiles are measured across 10–50 m range in 0.25–1 m increments, respectively. Additionally, information can be obtained about [near-bottom] temperature, but also about the sea-surface height, wind and surface waves when sampling from the bottom beyond the water depth (Visbeck and Fischer, 1995; Zedel, 2001; van Haren, 2001). This makes the instrument a versatile stand-alone tool. However, information on such environmental quantities needs to be distinguished from unexpected erroneous signals, such as those affecting ADCP's compass and echo intensity.

In an attempt to calibrate echo intensity data for a study on sediment transport in a tidal channel, extremely spiky data were found in the near-surface range of a bottom-mounted ADCP. In this note, it will be shown that the spikes reflect bubble clouds entrained by a ferry, which passed the mooring at close range regularly. The ferry was involved in the ADCP calibrations, because it carries a similar instrument in its hull. The functioning of this instrument was not affected by bubbles. Knowledge of the relative contribution of air bubbles to echo intensity is important, as studies on resuspension of material and estimation of atmospheric parameters using ADCP are hampered by injections of air bubbles reaching the bottom in shallow seas (Thorpe, 1986; van Haren, 2001).

As will also be demonstrated here, heading data from ADCP's compass can be used to monitor additional information that is used to compute currents. Heading variations can be affected by an ADCP-mooring moved around by currents, but the earth's magnetic field can also be disturbed by elements such as passing ships. Compass and motion-sensors output their data separately: heading and tilt, respectively. These data are internally used as knowledge of beams orientation, possibly varying with time which is necessary for current computation when ensemble averages of more than one acoustic ping are stored. Such computation can only be performed meaningfully in an orthogonal, Cartesian system like $[u, v, w]$, so that this knowledge is required even when the ADCP's output is in the non-orthogonal 'beam-coordinates'.

Correctly computed currents thus depend on the proper calibration of these sensors. The ADCP's fluxgate compass depends on *in situ* calibration more than on correct factory calibration. It can be de-oriented by magnetic metals in the mooring setup, or by other materials deflecting the earth's magnetic field. Large bodies of notably iron may influence the heading over distances 0 (10 m), as was already known in the days

E-mail address: hans.van.haren@nioz.nl

of Thomson Kelvin (1889). While a static calibration may be feasible, a dynamic one seems impossible, accounting for unwanted heading variations with time.

2. Data

A single flat $3 \times 1\,m^2$ bottom-frame was moored between 28 and 31 May 2001 at 52°59.025′N, 04°46.876′E, $H = 23\,m$ water depth, in the Marsdiep, the 4.5-km-wide sea-strait between the island of Texel and the mainland of the Netherlands (Fig. 1). The mooring was part of the regular calibration program of the island-ferry's ADCP. Every day, the ferry, 110 m long, 18 m wide, 4 m maximum draught, 3800 BRT, passed the mooring at a shortest distance of $200 \pm 150\,m$ twice per hour between 04:15 and 19:45 UTC. The bottom-frame was attached via chains and a cable to a second weight about 100 m away that lead to a surface marker. Besides several other sensors (not discussed here), the frame held an upward-looking 300 kHz broadband RDI-ADCP at 0.42 m above the bottom and a SeaBird SBE-26 bottom-pressure recorder at 0.08 m above the bottom. The ADCP sampled 50 vertical bins at mutual distances of $\Delta d = 0.5\,m$, storing single ping-data every 1.85 s. The bottom-pressure recorder sampled at 4 Hz, storing 2000 data-points before 100 s rest, every 10 min (600 s) period.

3. Observations

3.1. Bubble clouds entrained by a ferry

The echo intensity I is a measure for acoustic backscatter, which for a 300 kHz ADCP is sensitive to particles of a few mm and larger. This includes suspended sediment and zooplankton, but also air bubbles. Raw $I(z)$ need corrections for sound attenuation through the water column, before being compared, e.g., with samples of suspended material concentrations. For these corrections, general formulae depending on the transmit frequency (Urick, 1983; RDI, 1996) may be used, when an uncertainty of

about 10% is acceptable. Here, raw data are corrected by subtracting per depth level time mean $\langle I \rangle$ from the record, resulting in relative $dI(z) = I - \langle I \rangle$.

A typical depth–time series of dI in the Marsdiep shows regular semidiurnal tidal variations decreasing downward from the surface and likewise periodic semi- and fourth-diurnal variations decreasing upward from the bottom (Fig. 2a). The latter dI are associated with friction of the tidal currents, which are mainly in East–West U-direction and which have amplitudes exceeding $1\,m\,s^{-1}$ (Fig. 2b). These dI have a range of 30 dB and correspond with suspended matter concentrations varying between 10 and $100\,g\,m^{-3}$ (Fig. 2c). High suspended matter loads reach more than 15 m above the bottom (Fig. 3, dotted line). The weakly decreasing values with distance from the bottom indicate vigorous tidal mixing. Only in the upper 5 m the suspended matter concentration decreases substantially, in this example.

In the Marsdiep, near-surface semidiurnal tidal dI-variations of similar amplitudes to near-bottom dI are related to the advection of higher suspended matter loads by the ebb-flow from the fresher tidal flats Wadden Sea, thereby creating stratification. Both suspended material loads on dI are comparable with those by bubbles injected by surface waves in long-fetch shelf seas like the North Sea (Thorpe, 1986; van Haren, 2001). Near-surface dI may also be enhanced by foam lines delineating differently moving water masses. Most conspicuous in the present near-surface dI-records are the spikes superposed on the tidally varying, presumably resuspended sediment, concentrations (Fig. 2c). The half-hourly spikes reflect bubble clouds entrained by the Texel ferry passing the mooring.

That the ferry causes these spikes is inferred from the passages of heavy turbulence and foam lines in the wake of the ferry, which remain visible at the surface for about 5 min. The bubbles are generated in the hull and propellers wake and some by the displacement at the bow and along the sides of the ship. Apparently they are not drawn under the ship, possibly because of the particular Voith-Schneider cycloidal propulsion, as the ship's ADCP-data are not degraded by bubbles. Thus, a line of bubbles behind the ship marks its trajectory. This bubble wake has a width of approximately 1.5 times the ship's width and is delineated by foam lines at the two edges. The initially straight foam lines and wake of bubbles, under straight sailing, are subsequently displaced by varying advective currents in the channel.

The interpretation of the ferry causing the near-surface dI-spikes is supported by the fact that the ferry is not operated during the night, between 20 and 04 UTC in summer, except for emergencies. Acoustic interference with the ferry's 1.5 MHz ADCP can be ruled out as a cause for the spiky data. Direct acoustic hits of the hull of the ferry are clearly visible in the dI-data and they occur only when the ferry passes directly over the ADCP, which was once in the record (not shown).

The ferry-induced bubble clouds are detectable, in all four beams, but only so when the tidal current advects them over the ADCP. They degrade near-surface current measurements of all three components, which are marked 'bad data' when bubble clouds pass. This marking 'bad data' is likely due to the associated large variations between echoes in the different beams. As most of the ferry passages were to the east of the mooring (Fig. 1), nearly all ferry-induced dI-spikes are found during ebb-tide (Fig. 2). Thereby, bubble clouds can reach down to 18 m below the surface (Fig. 3). The decrease with depth is essentially linear, so that the scattering cross section decreases exponentially with depth, like in wave injected bubble clouds (Thorpe, 1986). The bubbles injected by the ferry enhance dI up to 30 dB close to the surface. This enhancement is comparable to the near-surface dI-increase during heavy storms in the North Sea (van Haren, 2001). It is
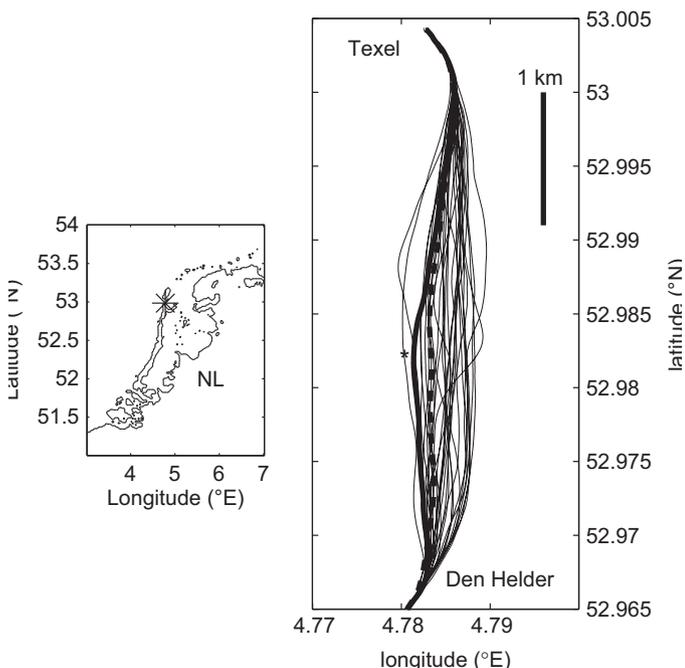

Fig. 1. Marsdiep (*) with 0-m line contouring the low-lying Netherlands (NL) and detail with mooring location (*) and ferry tracks on day 148, 2001. Heavy solid is track for Fig. 5, heavy dashed for Fig. 6.
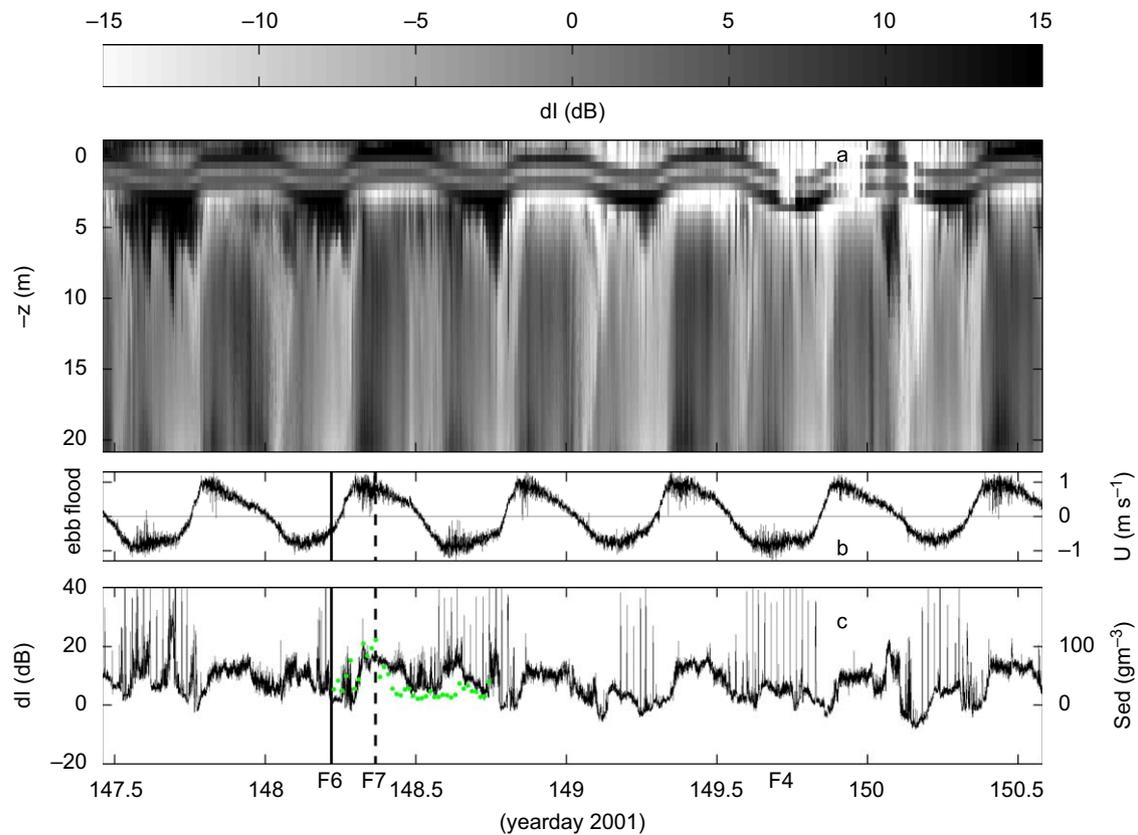
Fig. 2. Entire time series of (a) corrected, relative echo intensity *dI* of ADCP's beam ♯1 with depth. Note the double-hit of the sea-surface, which varies its level with semidiurnal tidal period. (b) Dominant east–west current, (c) near-surface, 7 m, *dI*, with suspended sediment from water samples on day 148 (green dots, scale to right). Vertical solid line indicates moment of Fig. 5, dashed line that of Fig. 6. Time is in year-days, with 12.00 UTC at January 1, 2001 = year-day 0.5.
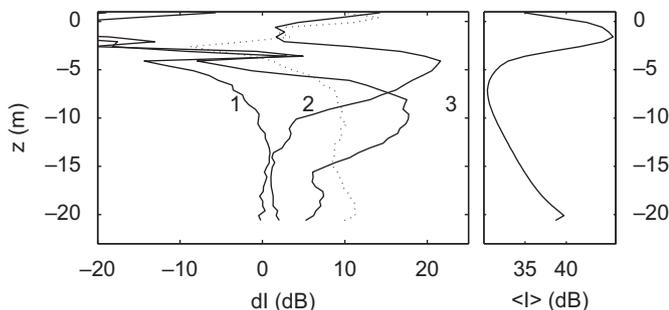

Fig. 3. Three profiles of *dI* with depth (labeled 1–3), before (1) and after (2, 3) the passage of a ferry on day 149.732 (solid lines). For comparison, the dotted line represents a profile when suspended bottom-material concentrations are high, on day 150.428. In the smaller panel to the right, the time mean echo intensity profile is given, which includes attenuation through the water column.

noted that such scattering is non-resonant for our relatively high-frequency ADCP (Polonichko, 1998) and that the bubbles have scattering cross-sections comparable to suspended matter loads reaching $100 \, \mathrm{g \, m^{-3}}$, as observed at this site near the bottom.

The entrainment of air bubbles by the ferry raises the intriguing possibility of observing bias in sea level estimation, via echo intensity, associated with bubbles in the water column. This is important, because the precise location of sea level is imperative for proper quantification of variations in atmospheric parameters on a bottom-mounted ADCP. Using ADCP-data that are sampled well beyond the sea surface from below, the surface location is found by fitting a parabola to the *dI(z)*-profile (Visbeck and Fischer, 1995) or by searching for the zero-crossing of *dI*'s vertical derivative yielding an accuracy of 0.03 m in sea level estimate (van Haren, 2001).

When the sea state is calm, as in the present Marsdiep observations, our broadband ADCP shows two peaks in *dI* 2 m apart due to reflection at the surface. This double-hit is due to the lag length between the two acoustic wave-groups of a ping $L_l = 1.42 \, \mathrm{m} > \Delta d$ > wave-group size (0.22 m), thus providing a transmission length of 1.87 m. As a result, an acoustically hard object like a sea surface is sensed in two different bins (L. Gostiaux, pers. comm.). This is observed in profiles like ♯1 of Fig. 3. As soon as bubble clouds appear, profile ♯2, the double-hit is masked. Worse, the main hit is found below the sea surface, by up to several *m*.

3.2. Compass-deviations induced by a ferry

Independent observations of measurement disturbances due to the ferry are obtained from occasionally large deviations in the ADCP's compass (Fig. 4). In principle the mooring-frame remains in position due to its weight of about 300 kg and the compass' heading normally does not vary more than $\pm 0.1°$, due to mooring vibrations, around its mean $\langle h \rangle = 151.0°$. However, spiky deviations of up to $\pm 10°$ are observed with a duration of about 25 s, well-resolved by the 0.55-Hz sampling (Figs. 5 and 6). These spikes are only observed in heading, not in tilt data (Figs. 4c, 5c, 6c). The latter do show some spikes, simultaneous with smaller spikes in heading, but these exclusively occur during moments in time of maximum [flood] current (Fig. 2b).

The heading-only spikes do not coincide with all ferry passages, *x* in Fig. 4b, there are much more near-surface *dI*-spikes than compass spikes, compare Fig. 4a with b. The heading spikes only occur when the ferry passes relatively close to the mooring, measurable up to 150 m distance under small wave conditions
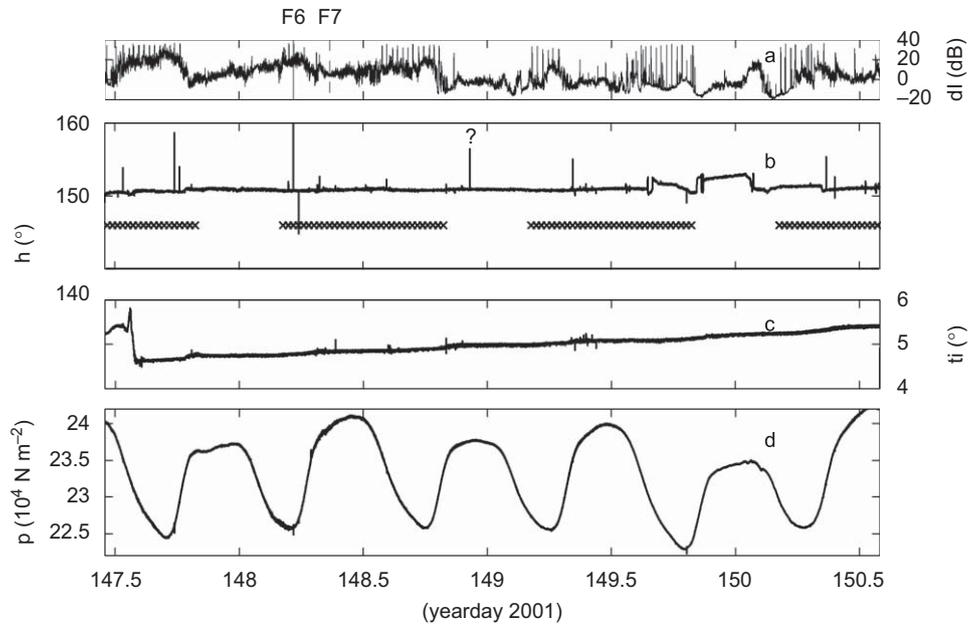
Fig. 4. Total time series of (a) near-surface, 5 m, *dl*, (b) ADCP-heading with *x* indicating each scheduled moment of ferry passage closest to the ADCP-site, (c) ADCP-tilt, (d) bottom pressure.
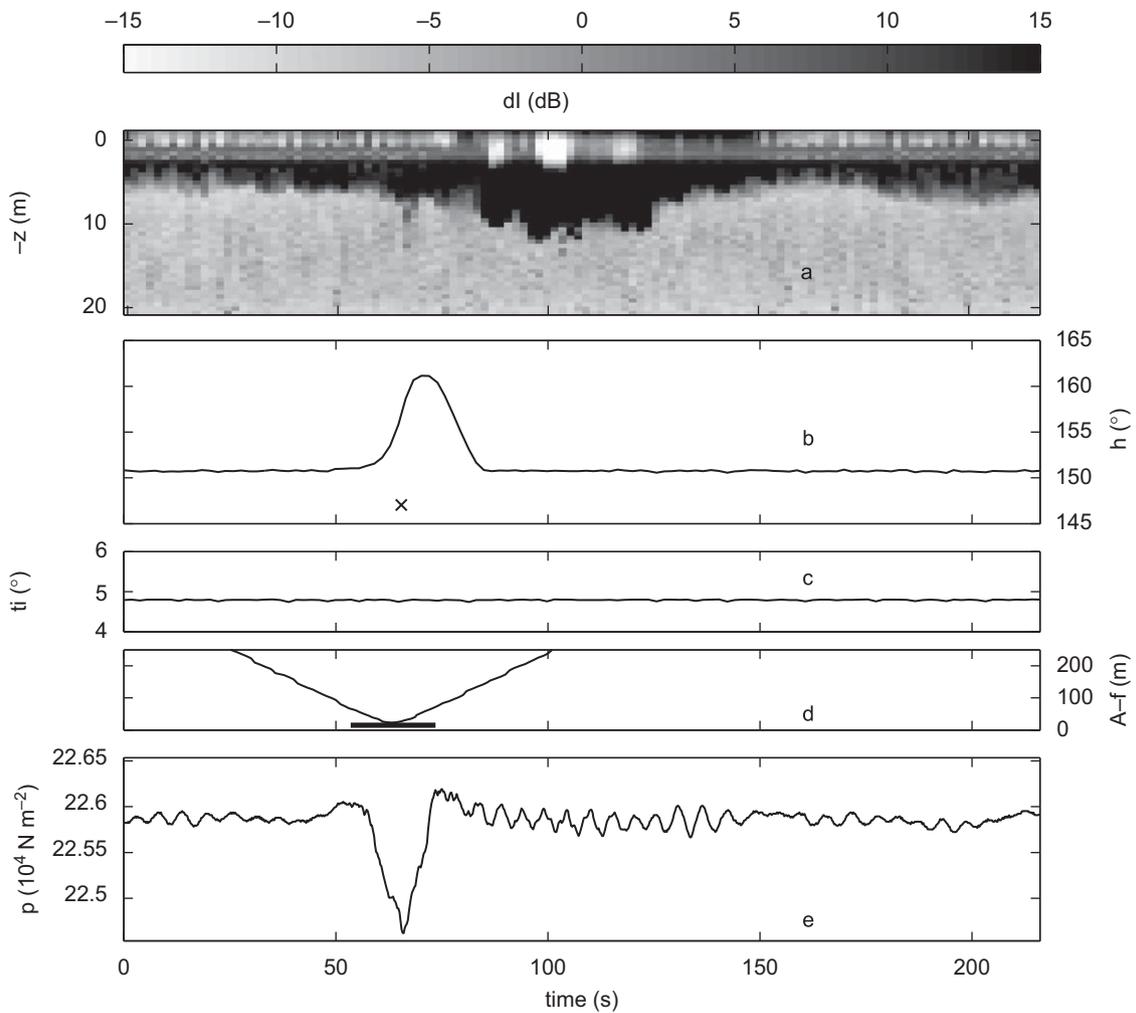

Fig. 5. Detail time series, with starting day 148.2180, during ebb-flow and ferry transit Den Helder→Texel, on time. (a) Relative echo with depth, (b) ADCP-heading with x indicating scheduled moment of ferry passage closest to the ADCP-site, (c) ADCP-tilt, (d) distance ADCP–ferry is measured using ship's GPS and corrected to indicate the centre of the ferry. The ferry sails at about 6 m s^{-1}, so that it takes 18 s between front and rear to pass. The horizontal bar indicates the approximate length of the ferry, assuming it sails at constant speed, at the moment when its centre passes the mooring at shortest distance. (e) Bottom pressure.
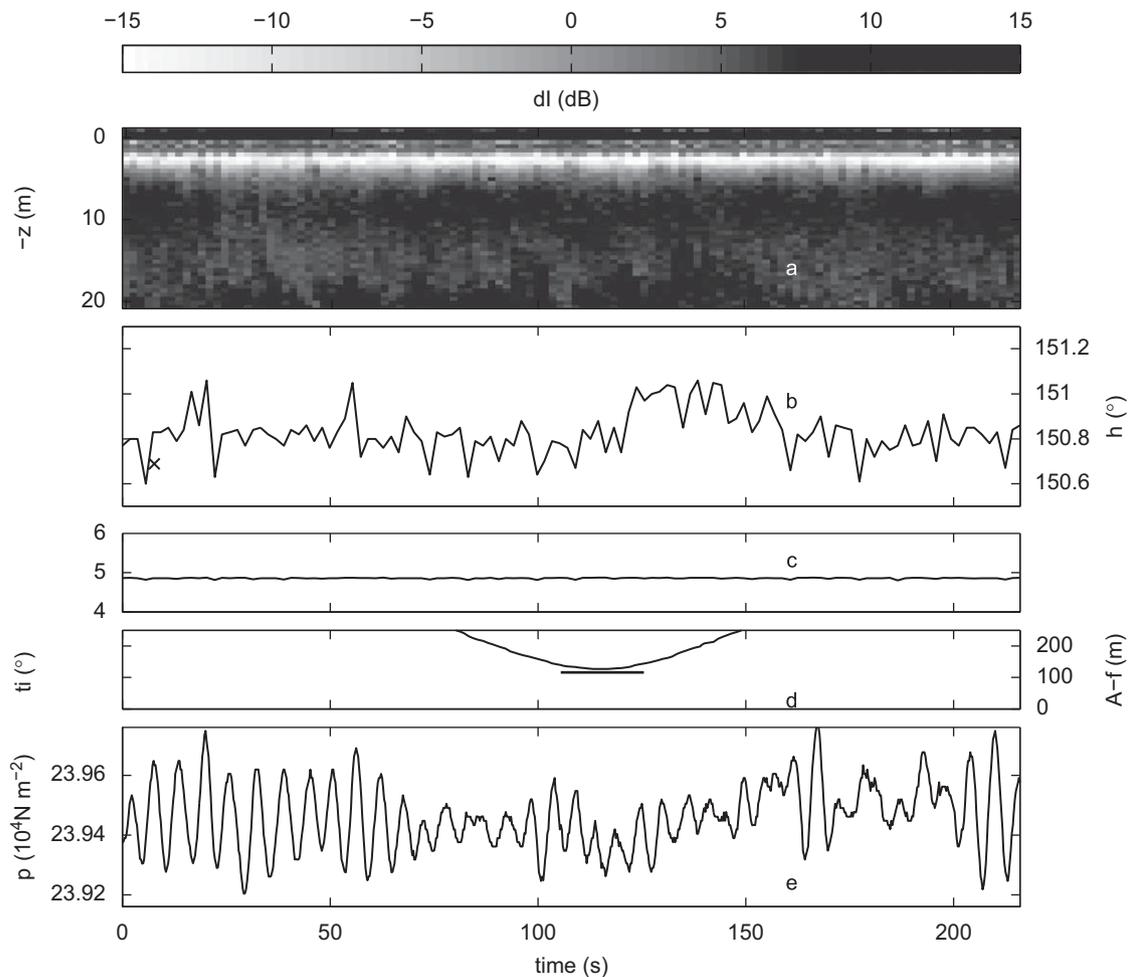
Fig. 6. As Fig. 5, but with starting day 148.3645, during strong flood-flow and ferry Texel→Den Helder sailing about 2 min late. Note different vertical scales in (b) and (e), compared to Fig. 5b and e, respectively.

(Fig. 6). Upon such relatively far-away passage, bubble clouds spread over a wider range in the *dI*-record as they are longer advected by tidal currents after the ferry's passage, compared to a near or overhead passage (Fig. 5).

Although bubble clouds decrease intensity over time, their advection by the tidal current makes them less suitable for estimating distance A–f between ADCP "A" and ferry "f". Heading variations however, are clear, non-linear, functions of A–f. This can be inferred from a single passage, e.g., (Fig. 5d), or from several passages at different distances, compare Fig. 5 (~20 m distance) with Fig. 6 (126 m distance). It shows that the compass 'spikes' are directly associated with the stern of the ship, presumably the rotating impellors, affecting the earth's magnetic field most. This is inferred from timing with respect to the ship's passage. The compass spikes also indicate whether the ferry passes to the east or west of the ADCP: as the compass orientation is fixed to magnetic North, an easterly passage of an attracting disturbance will pull the compass 'needle' to the east. This adds value to the compass reading, hence a positive disturbance in the record. The majority of spikes is positive, commensurate the majority of east-side passages.

3.3. Bottom-pressure variations by a ferry

A nearby ferry-passing is also evidenced in bottom-pressure data, showing solitary non-surface wave depressions when spikes in compass deviation occur (Figs. 4e, 5e, 6e). The persistent dip in

pressure, surrounded by weaker rises on either side, corresponds well with a model of the typical bottom pressure of a moving vessel (Lazauskas, 2007). This includes pressure being sensed laterally much further than twice the vessel's width, more like its length away, and the pressure dip being observed simultaneously with passage of the centre of the ship. The observed depression is $0.1–1.2 \times 10^3 \, \mathrm{N\,m^{-2}}$, equivalent to 0.01–0.12 m water level, for passages at 126 m (Fig. 6) and 22 m (Fig. 5), respectively.

4. Discussion

It may be clear that a 10° heading variation by a ferry has non-negligible effect on current observations using a bottom-mounted ADCP, but the regular short duration of the ferry's passage will not pose large effects on the measurement of tidal current. However, more often irregular passages of unknown ships may pose some problems, as these are less well recognizable in the data, just like mooring-line sways. As the Texel ferry's heading and bottom-pressure variations signature is a 25-s passage (Figs. 5 and 6), the unidentified 100-s heading peak in the night on day 148.913 (Fig. 4b) is from a different ship passing over our mooring. Such information is used in mine warfare (anonymous, 2009). Nevertheless, although each of the effects by the ferry can be easily detected, other ships passing irregularly the mooring-site are not always as well recognizable. This is also because ship-induced variations are comparable to those generated by high-frequency

turbulence and internal waves. In estuaries and sea straits like the Marsdiep, the latter typically have periods of 30–120 s, which is similar to the duration of a ship's passage. In such areas the ship's rapid bottom-pressure variations exceed those induced by surface waves, being more typical of open sea waves under moderate wind conditions.

Naturally, for high-frequency sampling as in Reynolds stress estimates using ADCP (e.g., Howarth and Souza, 2005), such ship-induced pulses must be resolved prior to momentum flux computations. On the other hand, the present observations may be used advantageously, e.g., to calibrate echo intensity against bubble clouds or compare ship's wake data with wind-induced data. As a final remark, the bubbles did not affect measurements using this ferry's ADCP that was mounted centrally, but this may not hold for other ships with different propulsion, hull form and ADCP-mounting.

Acknowledgments

References

anonymous, 2009. Underwater weapons. ⟨http://www.fas.org/amn/dod-101/navy/docs/es310/uw_wpns/uw_wpns.htm⟩.

Howarth, M.J., Souza, A.J., 2005. Reynolds stress observations in continental shelf seas. Deep Sea Research II 52, 1075–1086.

Lazauskas, L., 2007. The hydrodynamic resistance, wave wakes and bottom pressure signatures of a 5900 t displacement air warfare destroyer. Int. rep. Department Appl. Math. University Adelaide, Adelaide. ⟨http://www.cyberiad.net/library/pdf/nibberluna0.pdf⟩.

Polonichko, V., 1998. Response of the upper ocean to wind, wave and buoyancy forcing. PhD Thesis, University of Victoria, Victoria, BC.

RDI, 1996. Acoustic Doppler Current Profiler, Principles of Operation, A Practical Primer. RDI, San Diego.

Thomson Kelvin, W., 1889. On the security against disturbances of ships' compasses by electric lighting appliances. Mathematical and Physical papers, Vol. 5, paper 219, Cambridge University Press (1911), 474–480.

Thorpe, S.A., 1986. Measurements with an automatically recording inverted echo sounder; ARIES and the bubble clouds. Journal of Physical Oceanography 16, 1462–1478.

Urick, R.J., 1983. Principles of Underwater Sound. McGraw-Hill.

van Haren, H., 2001. Estimates of sea level, waves and winds from a bottom-mounted ADCP in a shelf sea. Journal of Sea Research 45, 1–14.

Visbeck, M., Fischer, J., 1995. Sea surface conditions remotely sensed by upward-looking ADCPs. Journal of Atmospheric and Oceanic Technology 12, 141–149.

Zedel, L., 2001. Using ADCP background sound levels to estimate wind speed. Journal of Atmospheric and Oceanic Technology 12, 1867–1881.